GVKLG sequence in the seventh transmembrane domain, which could be involved in their interaction with APH-1.

We previously identified a human APH-1b splice variant lacking the entire fourth transmembrane domain. We found that the variant protein is present at much lower levels than the wild-type APH-1b in transiently transfected cells but that it can interact with exogenous nicastrin (Saito et al., 2005). Consistent with this finding, co-immunoprecipitation revealed that exogenous nicastrin can interact with the mutant APH-1aL (data not shown). We also found that exogenous APH-1aS augmented the levels of immature nicastrin in PS-deficient cells. Thus, APH-1 seems to interact with immature nicastrin at a site other than the fourth transmembrane domain. These results are in accord with recent studies showing that wild-type as well as Gly mutant APH-1 interact with nicastrin in *Drosophila* cells (Niimura et al., 2005) and that nicastrin can interact with APH-1 C-terminal fragments produced by cleavage downstream of the fourth transmembrane domain (Fortna et al., 2004).

In the present study, we generated the first antibody to the C-terminus of APH-1aS. This antibody can specifically detect overexpressed APH-1aS. As shown in Fig. 5, this antibody is also useful for distinguishing between endogenous APH-1aS and APH-1aL, although it has weak crossreactivity with APH-1aL. Generation of more sensitive and specific APH-1aS antibodies should help compare the functional significance of APH-1aS and APH-1aL.

In summary, our present characterization of APH-1 mutants with a disrupted GxxxG motif indicates that this region plays a crucial role in the stability of the APH-1 protein as well as in the assembly of PS complexes. Further clarification of the interaction of APH-1 with nicastrin and PSs and determination of the stoichiometry of individual components in the PS complex will help elucidate the molecular mechanisms by which γ-secretase

cleaves transmembrane proteins and generates Aβ.

Acknowledgements.

We are grateful to Dr. Bart De Strooper for the supply of wild-type and PS-knockout fibroblasts, Ms. Yumiko Ishii and Kimiko Shimoji for technical assistance, Dr. Taisuke Tomita for helpful suggestions, and Dr. Takeshi Tabira for his assistances. This work was supported in part by grants from the Ministry of Health, Labor and Welfare of Japan and by the Organization for Pharmaceutical Safety and Research, Japan.

References

Araki W., Yuasa K., Takeda S., Takeda K., Shirotani K., Takahashi K. et al. (2001) Pro-apopototic effect of presenilin 2 (PS2) overexpression is associated with downregulation of Bcl-2 in cultured neurons. *J. Neurochem.* **79,** 1161-1168.

Chui D.H., Shirotani K., Tanahashi H., Akiyama H., Ozawa K., Kunishita T. et al. (1998) Both N-terminal and C-terminal fragments of presenilin 1 colocalize with neurofibrillary tangles in neurons and dystrophic neurites of senile plaques in Alzheimer's disease. *J. Neurosci. Res.* **53,** 99-106.

Citron M., Westaway D., Xia W., Carlson G., Diehl T., Levesque G. et al. (1997) Mutant presenilins of Alzheimer's disease increase production of 42-residue amyloid beta-protein in both transfected cells and transgenic mice. *Nat. Med.* **3,** 67-72.

Edbauer D., Winkler E., Regula J.T., Pesold B., Steiner H. and Haass C. (2003) Reconstitution of gamma-secretase activity. *Nat. Cell Biol.* **5,** 486-488.

Edbauer D., Kaether C., Steiner H. and Haass C. (2004) Co-expression of nicastrin and presenilin rescues a loss of function mutant of APH-1. *J. Biol. Chem.* **279,** 37311-37315.

Ephrat L.-L., Wasco W., Poorkaj P., Romano D.M., Oshima J., Pettingell W.H. et al. (1995) Candidate gene for the chromosome 1 familial Alzheimer's disease locus. *Science* **269,** 973-977.

Fortna R.R., Crystal A.S., Morais V.A., Pijak D.S., Lee V.M.and Doms R.W. (2004) Membrane topology and nicastrin-enhanced endoproteolysis of APH-1, a component of the gamma-secretase complex. *J. Biol. Chem.* **279,** 3685-3693.

Francis R., McGrath G., Zhang J., Ruddy D.A., Sym M., Apfeld J. et al. (2002) aph-1 and pen-2 are required for Notch pathway signaling, gamma-secretase cleavage of betaAPP, and presenilin protein accumulation. *Dev. Cell* **3,** 85-97.

Goutte C., Tsunozaki M., Hale V.A. and Priess J.R. (2002) APH-1 is a multipass membrane protein essential for the Notch signaling pathway in Caenorhabditis elegans embryos. *Proc. Natl. Acad. Sci. USA* **99,** 775-779.

Gu Y., Chen F., Sanjo N., Kawarai T., Hasegawa H., Duthie M. et al. (2003) APH-1 interacts with mature and immature forms of presenilins and nicastrin and may play a role in maturation of presenilin.nicastrin complexes. *J. Biol. Chem.* **278,** 7374-7380.

Herreman A., Serneels L., Annaert W., Collen D., Schoonjans L. and De Strooper B. (2000) Total inactivation of gamma-secretase activity in presenilin-deficient embryonic stem cells. *Nat. Cell Biol.* **2,** 461-462.

Hu Y. and Fortini M.E. (2003) Different cofactor activities in gamma-secretase assembly: evidence for a nicastrin-Aph-1 subcomplex. *J. Cell Biol.* **161,** 685-690.

Kimberly W.T. and Wolfe M.S. (2003) Identity and function of gamma-secretase. *J. Neurosci. Res.* **74,** 353-360.

Kimberly W.T., LaVoie M.J., Ostaszewski B.L., Ye W., Wolfe M.S. and Selkoe D.J. (2003) Gamma-secretase is a membrane protein complex comprised of presenilin, nicastrin, Aph-1, and Pen-2. *Proc. Natl. Acad. Sci. USA* **100,** 6382-6387.

LaVoie M.J., Fraering P.C., Ostaszewski B.L., Ye W., Kimberly W.T., Wolfe M.S. et al. (2003) Assembly of the gamma-secretase complex involves early formation of an intermediate subcomplex of Aph-1 and nicastrin. *J. Biol. Chem.* **278,** 37213-37222.

Lee S.F., Shah S., Li H., Yu C., Han W. and Yu G. (2002) Mammalian APH-1 interacts with presenilin and nicastrin and is required for intramembrane proteolysis of amyloid-beta precursor protein and Notch. *J. Biol. Chem.* **277,** 45013-45019.

Lee S.F., Shah S., Yu C., Wigley W.C., Li H., Lim M. et al. (2004) A conserved GXXXG motif in APH-1 is critical for assembly and activity of the gamma-secretase complex. *J. Biol. Chem.* **279,** 4144-4152.

Ma G., Li T., Price D.L. and Wong P.C. (2005) APH-1a is the principal mammalian APH-1 isoform present in gamma-secretase complexes during embryonic development. *J. Neurosci.* **25,** 192-198.

Morais V.A., Crystal A.S., Pijak D.S., Carlin D., Costa J., Lee V.M. et al. (2003) The transmembrane domain region of nicastrin mediates direct interactions with APH-1 and the gamma-secretase complex. *J. Biol. Chem.* **278,** 43284-43291.

Niimura M., Isoo N., Takasugi N., Tsuruoka M., Ui-Tei K., Saigo K. et al. (2005) Aph-1 contributes to the stabilization and trafficking of the gamma-secretase complex through mechanisms involving intermolecular and intramolecular interactions. *J. Biol. Chem.* **280,** 12967-12975.

Russ W.P. and Engelman D.M. (2000) The GxxxG motif: a framework for transmembrane helix-helix association. *J. Mol. Biol.* **296,** 911-919.

Saito S. and Araki W. (2005) Expression profiles of two human APH-1 genes and their roles in the formation of presenilin complexes.*Biochem. Biophys. Res. Comm.* **327,** 18-22.

Saito S., Takahasi-Sasaki N. and Araki W. (2005) Identification and characterization of a novel human APH-1b splice variant lacking exon 4. *Biochem. Biophys. Res. Comm.* **330,** 1068-1072.

Sebastien S., Hebert S.S., Serneels L. Dejaegere T., Horre K., Dabrowski M. et al. (2004) Coordinated and widespread expression of gamma-secretase in vivo: evidence for size and molecular heterogeneity. *Neurobiol. Dis.* **17,** 260-272.

Serneels L., Dejaegere T., Craessaerts K., Horre K., Jorissen E., Tousseyn T. et al. (2005) Differential contribution of the three Aph1 genes to gamma-secretase activity in vivo. *Proc. Natl. Acad. Sci. USA* **102,** 1719-1724.

Sherrington R., Rogaev E.I., Liang Y., Rogaeva E.A., Levesque G., Ikeda M. et al. (1995) Cloning of a gene bearing missense mutations in early-onset familial Alzheimer's disease. *Nature* **375,** 754-760.

Shiraishi H., Sai X., Wang H.Q., Maeda Y., Kurono Y., Nishimura M. et al. (2004) PEN-2 enhances gamma-cleavage after presenilin heterodimer formation. *J. Neurochem.* **90,** 1402-1413.

Shirotani K., Takahashi K. and Tabira T. (1999) Determination of a cleavage site of presenilin 2 protein in stably transfected SH-SY5Y human neuroblastoma cell lines. *Biochem. Biophys. Res. Commun.* **240,** 728-731.

Shirotani K., Takahashi K., Araki W., Maruyama K. and Tabira T. (2000) Mutational analysis of intrinsic regions of presenilin 2 that determine its endoproteolytic cleavage and pathological function. *J. Biol. Chem.* **275,** 3681-3686.

Shirotani K., Edbauer D., Prokop S., Haass C. and Steiner H. (2004a) Identification of distinct gamma-secretase complexes with different APH-1 variants. *J. Biol. Chem.* **279,** 41340-41345.

Shirotani K., Edbauer D., Kostka M., Steiner H. and Haass C. (2004b) Immature nicastrin stabilizes APH-1 independent of PEN-2 and presenilin: identification of nicastrin mutants that selectively interact with APH-1. *J. Neurochem.* **89,** 1520-1527.

Sisodia S.S. and St George-Hyslop P.H. (2002) gamma-Secretase, Notch, Abeta and Alzheimer's disease: where do the presenilins fit in? *Nat. Rev. Neurosci.* **3,** 281-290.

Takasugi N., Tomita T., Hayashi I., Tsuruoka M., Niimura M., Takahashi Y. et al. (2003) The role of presenilin cofactors in the gamma-secretase complex. *Nature* **422,** 438-441.

Thinakaran G., Borchelt D.R., Lee M.K., Slunt H.H., Spitzer L., Kim G. et al. (1996) Endoproteolysis of presenilin 1 and accumulation of processed derivatives in vivo. *Neuron* **17**, 181-190.

Yu G., Nishimura M., Arawaka S., Levitan D., Zhang L., Tandon A. et al. (2000) Nicastrin modulates presenilin-mediated notch/glp-1 signal transduction and betaAPP processing. *Nature* **407**, 48-54.

Figure Legends

Fig. 1.

(A) Schematic diagrams of the structures of APH-1aS, APH-1aL, and APH-1b. APH-1aS, APH-1aL, and APH-1b have seven transmembrane domains (dotted boxes). The fourth transmembrane domain contains a conserved GxxxG motif. APH-1aS and APH-1aL have different C-termini (indicated by gray boxes) due to alternative splicing. The underlined portions indicate the amino acid residues used to generate specific antibodies. aa, amino acids. **(B)** Partial amino acid sequences of human and *C. elegans* APH-1. Human APH-1a and APH-1b and *C. elegans* APH-1 have a conserved GxxxG motif in their fourth putative transmembrane domains. Human APH-1 contains a tandem GxxxG sequence.

Fig. 2. Effects of APH-1aS or APH-1b overexpression on endogenous expression of APH-1aL.

(A) HEK293 (293) or HeLa cells were transiently transfected with empty vector or vectors containing APH-1aS or APH-1b DNA, and expression of endogenous APH-1aL was examined by Western blotting with an anti-APH-1aL antibody (O2C2). Overexpressed APH-1aS and APH-1b were analyzed by Western blotting with anti-APH-1aS and anti-APH-1b antibodies, respectively. Asterisks indicate nonspecific signals. **(B)** HeLa cells were transiently transfected with varying amounts of APH-1aS cDNA, and endogenous APH-1aL and exogenous APH-1aS were examined as in A. Equal amounts of DNA were transfected by addition of vector DNA. **(C)** Wild-type (WT) and PS-knockout (dKO) fibroblasts were infected with a retroviral vector, pMX (Vec) or pMX-APH-1aS (aS). Expressions of endogenous APH-1aL and exogenous APH-1aS were analyzed as in A. Endogenous expression of nicastrin, PS1, and PS2 were also assessed by Western blotting with relevant antibodies. Mature nicastrin (mNIC), PS1

N-terminal fragments (NTF), and PS2 C-terminal fragments (CTF) were undetectable in PS-deficient cells. iNIC, immature nicastrin. Each figure is a representative of at least two independent experiments, which gave essentially identical results.

Fig. 3. Reduced expression of G122D and L123D APH-1aL mutants in transiently transfected cells.

(A) HeLa or HEK293 cells were transiently transfected with empty vector or vectors containing wild-type, G122D mutant, or L123D mutant APH-1aL cDNA. Cells were lysed in 1% CHAPSO buffer, and cell lysates were analyzed by Western blotting with an anti-APH-1aL antibody. APH-1aL protein bands are indicated by arrows. Non, non-transfected cells. **(B)** The intensities of the APH-1aL bands in A were quantified and used to calculate the relative protein levels. Data are represented as means of two independent experiments.

Fig. 4. Stability of wild-type and G122D mutant APH-1aL proteins.

(A) WT-APH-1aL cells (WT) and GD-APH-1aL cells (GD) were treated with 100 μg/ml cycloheximide (CHX) for the indicated times, and cell lysates were subjected to Western blotting with an anti-APH-1aL antibody as described in Fig. 3. APH-1aL protein bands are indicated by arrows. **(B)** The intensities of the bands in A were quantified and used to calculate the relative protein levels. Data are represented as means of two independent experiments.

Fig. 5. Wild-type but not G122D mutant APH-1aL is incorporated into PS1 complexes and downregulates endogenous APH-1aS expression.

(A) CHAPSO lysates from cells stably transfected with empty vector or wild-type (WT)

APH-1aL or G122D mutant (GD) APH-1aL cDNA were immunoprecipitated with anti-PS1 antibodies (PS1N62) and analyzed by immunoblot analysis with an anti-APH-1aL antibody (O2C2) or an anti-APH-1aS antibody. The membrane was reprobed with anti-PS1 antibody. **(B)** The intensities of APH-1aL bands in A were quantified and used to calculate the relative protein levels. Data are represented as means of two to three independent experiments.

Fig. 6. Schematic representation of the relationship between PS complexes and wild-type and mutant APH-1aL.

In vector-transfected cells (*Vec*), endogenous APH-1aS (aS) and APH-1aL (aL) are independently expressed as components of PS complexes (large circles). In wild-type APH-1aL-expressing cells (*WT*), overexpressed APH-1aL is incorporated into PS complexes, displacing endogenous APH-1aS. In contrast, in G122D mutant APH-1aL-exressing cells (*GD*), the overexpressed mutant APH-1aL (GD) is not incorporated into PS complexes and APH-1aS is not displaced, leading to rapid degradation of the mutant APH-1. APH-1b is omitted to simplify this figure.

Fig. 1

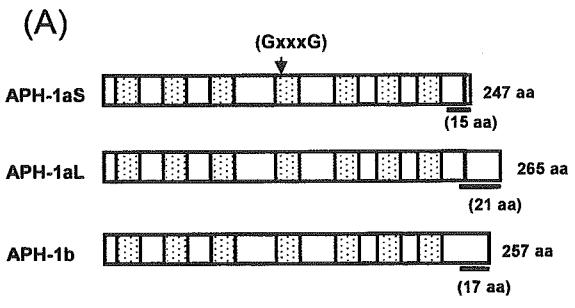
(A)
(GxxxG)
APH-1aS
247 aa
(15 aa)
APH-1aL
265 aa
(21 aa)
APH-1b
257 aa
(17 aa)
(B)
Human APH-1a 118 AYVSGLSFGIISGVFSV 134
Human APH-1b 117 AYVSGLGFGIMSGVFSF 133
C. elegans APH-1 119 ALVCGLGMGVISALFYT 135

Fig. 2

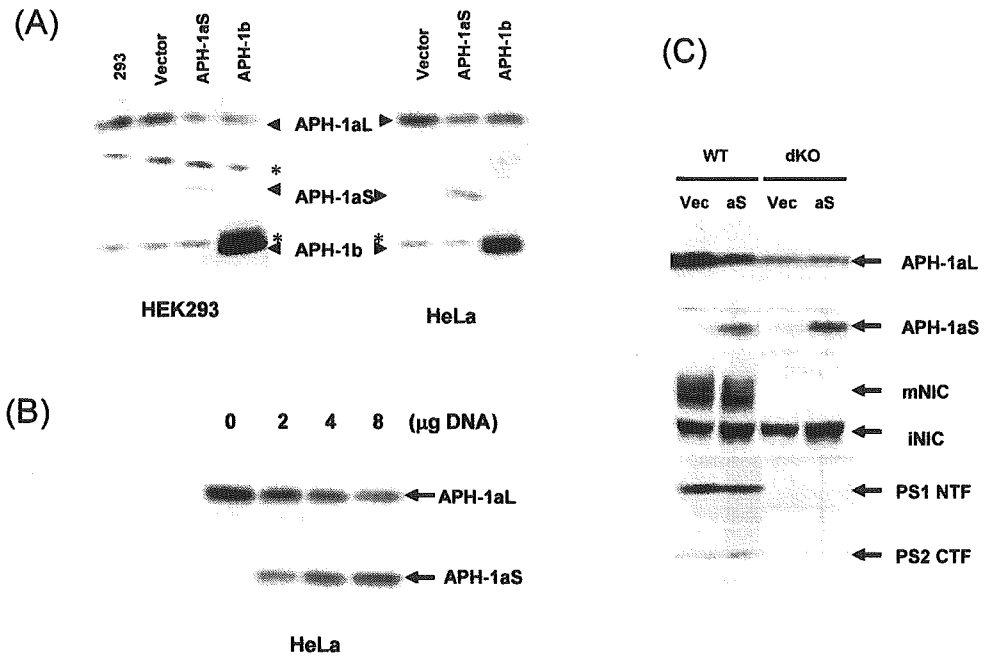
(A)
293
Vector
APH-1aS
APH-1b
Vector
APH-1aS
APH-1b
APH-1aL
APH-1aS
APH-1b
HEK293
HeLa
(B)
0
2
4
8
(μg DNA)
APH-1aL
APH-1aS
HeLa
(C)
WT
dKO
Vec
aS
Vec
aS
APH-1aL
APH-1aS
mNIC
iNIC
PS1 NTF
PS2 CTF

Fig. 3

(A)

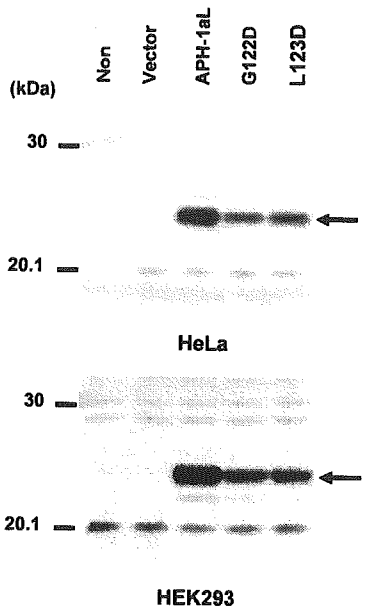
Non
Vector
APH-1aL
G122D
L123D
(kDa)
30
20.1
HeLa
30
20.1
HEK293

(B)

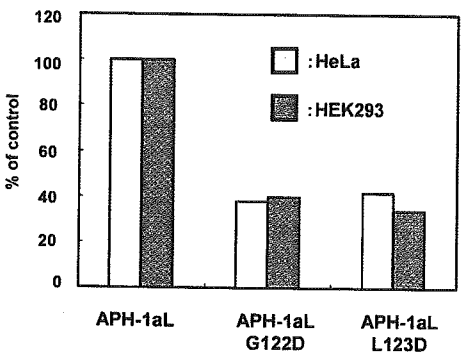
120
100
80
60
40
20
0
% of control
:HeLa
:HEK293
APH-1aL
APH-1aL G122D
APH-1aL L123D

Fig. 4

(A)

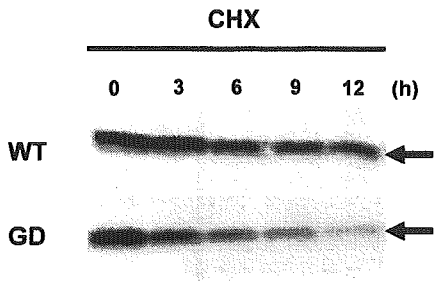
CHX
0
3
6
9
12
(h)
WT
GD

(B)

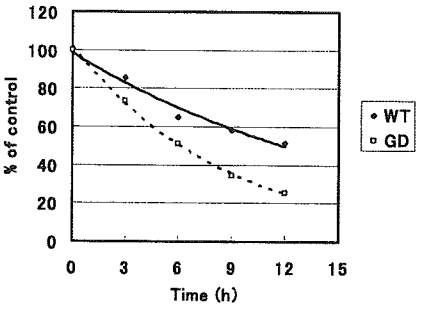
120
100
80
60
40
20
0
% of control
0
3
6
9
12
15
Time (h)
WT
GD

Fig. 5

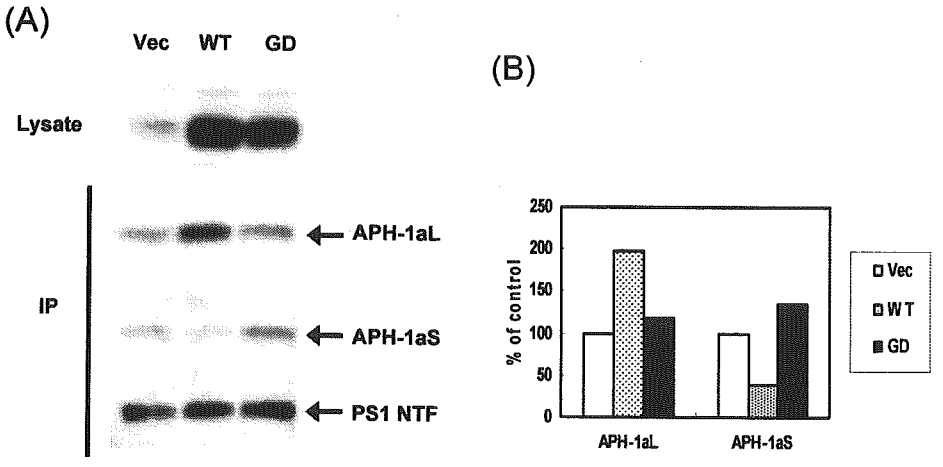
(A)
Vec
WT
GD
Lysate
IP
APH-1aL
APH-1aS
PS1 NTF
(B)
% of control
250
200
150
100
50
0
APH-1aL
APH-1aS
Vec
WT
GD

Fig. 6

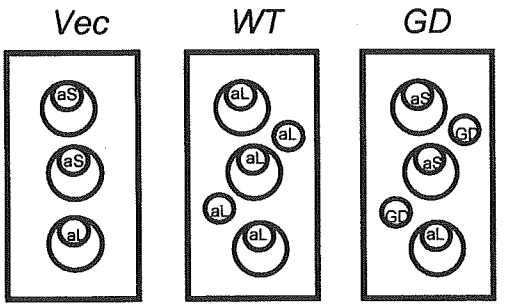

THE JOURNAL OF BIOLOGICAL CHEMISTRY
Vol. 280, No. 19, Issue of May 13, pp. 19070–19077, 2005
Printed in U.S.A.
© 2005 by The American Society for Biochemistry and Molecular Biology, Inc.

Random Mutagenesis of Presenilin-1 Identifies Novel Mutants Exclusively Generating Long Amyloid β-Peptides*

Received for publication, January 31, 2005, and in revised form, March 10, 2005
Published, JBC Papers in Press, March 10, 2005, DOI 10.1074/jbc.M501130200

Yoshifumi Nakaya‡§, Takuya Yamane‡, Hirohisa Shiraishi¶, Hua-Qin Wang‡, Etsuro Matsubara‖, Toru Sato, Georgia Dolios‡‡, Rong Wang‡‡, Bart De Strooper§§, Mikio Shoji‖, Hiroto Komano¶, Katsuhiko Yanagisawa¶, Yasuo Ihara**, Paul Fraser¶¶, Peter St George-Hyslop¶¶, and Masaki Nishimura‡‖‖**

*From the ‡Molecular Neuroscience Research Center, Shiga University of Medical Science, Shiga 520-2192, Japan, the §Department of Neurology, Kyoto University Graduate School of Medicine, Kyoto 606-8507, Japan, the ¶Department of Dementia Research, National Institute for Longevity Sciences, Aichi 474-8522, Japan, the ‖Department of Neurology, Okayama University Graduate School of Medicine and Density, Okayama 700-8558, Japan, the **Department of Neuropathology, Faculty of Medicine, University of Tokyo, Tokyo 113-0033, Japan, the ‡‡Department of Human Genetics, Mount Sinai School of Medicine, New York, New York 10029, the §§Center for Human Genetics, Katholieke Universiteit Leuven and Flanders Interuniversity Institute for Biotechnology, 3000 Leuven, Belgium, and the ¶¶Centre for Research in Neurodegenerative Diseases, University of Toronto, Toronto, Ontario M5S 3H2, Canada*

Familial Alzheimer disease-causing mutations in the presenilins increase production of longer pathogenic amyloid β-peptides ($A\beta_{42/43}$) by altering γ-secretase activity. The mechanism underlying this effect remains unknown, although it has been proposed that heteromeric macromolecular complexes containing presenilins mediate γ-secretase cleavage of the amyloid β-precursor protein. Using a random mutagenesis screen of presenilin-1 (PS1) for PS1 endoproteolysis-impairing mutations, we identified five unique mutants, including R278I-PS1 and L435H-PS1, that exclusively generated a high level of $A\beta_{43}$, but did not support physiological PS1 endoproteolysis or $A\beta_{40}$ generation. These mutants did not measurably alter the molecular size or subcellular localization of PS1 complexes. Pharmacological studies indicated that the up-regulation of activity for $A\beta_{43}$ generation by these mutations was not further enhanced by the difluoroketone inhibitor DFK167 and was refractory to inhibition by sulindac sulfide. These results suggest that PS1 mutations can lead to a wide spectrum of changes in the activity and specificity of γ-secretase and that the effects of PS1 mutations and γ-secretase inhibitors on the specificity are mediated through a common mechanism.

The amyloid β-precursor protein (APP),[1] Notch, ErbB-4, and several other unrelated type 1 transmembrane (TM) proteins undergo γ-secretase cleavage within their TM domains (1, 2). The consequential proteolytic release of the intracellular domains of these substrates has been revealed to be involved in signaling from the membrane to the nucleus (3). In the case of APP, γ-secretase mediates γ- and ε-cleavage to generate a heterogeneous series of N- and C-terminal products named the amyloid β-peptide (Aβ) and the APP intracellular domain (AICD), respectively. Aβ peptides have C termini that end at residue 38, 40, 42, or 43, whereas AICD fragments begin at residues 48–52 of the Aβ domain (4, 5). The process regulating these heterogeneous intramembranous cleavages is poorly understood, but is a central issue in Alzheimer disease research for three reasons. First, the longer Aβ species ending at residue 42 or 43 ($A\beta_{42/43}$) are thought to play a critical role in the pathogenesis of Alzheimer disease, although they are minor products of normal γ-secretase activity (6). Second, clinical mutations in the presenilins (PSs), which are responsible for the majority of familial Alzheimer disease (FAD) pedigrees, cause increased ratios of $A\beta_{42/43}$ isoforms to total Aβ (7). Third, medication that modulates $A\beta_{42/43}$ production by altering γ-secretase activity could provide an effective therapy for Alzheimer disease.

PS1 and PS2 are multipass TM proteins and undergo endoproteolysis within their large cytoplasmic loop domains by an unknown protease named presenilinase (8, 9). This endoproteolysis yields N-terminal (NTF) and C-terminal (CTF) fragments that are stabilized and assembled into functional macromolecular complexes together with at least three other membrane proteins, nicastrin, APH-1, and PEN-2 (10, 11). The abundance and stoichiometry of PS complexes are tightly regulated, and exogenously overexpressed PSs can replace endogenous PSs (8). Recent studies have suggested that these multiprotein complexes mediate γ-secretase cleavage and probably PS endoproteolysis and that PSs may be the catalytic components of the complexes (2, 12–15). Furthermore, it has been presumed that FAD-associated mutations of the PSs significantly alter γ-secretase activity and enhance production of $A\beta_{42/43}$ through a gain-of-function effect. However, it is still unclear how >100 of the FAD-linked missense mutations scat-

* This work was supported in part by a grant-in-aid for scientific research from the Ministry of Education, Culture, Sports, Science, and Technology of Japan (to M. N.); by grants from the Life Science Foundation and the Uehara Memorial Foundation (to M. N.), the Canadian Institutes of Health Research and Howard Hughes Medical Institute (to P. St G.-H.), and the Ontario Mental Health Foundation (to P. F.); and by National Institutes of Health Grant AG10491 (to R. W.). The costs of publication of this article were defrayed in part by the payment of page charges. This article must therefore be hereby marked "*advertisement*" in accordance with 18 U.S.C. Section 1734 solely to indicate this fact.

‖‖ To whom correspondence should be addressed: Molecular Neuroscience Research Center, Shiga University of Medical Science, Seta, Otsu, Shiga 520-2192, Japan. Tel.: 81-77-548-2327; Fax: 81-77-548-2402; E-mail: mnishimu@belle.shiga-med.ac.jp.

[1] The abbreviations used are: APP, amyloid β-precursor protein; TM, transmembrane; Aβ, amyloid β-peptide; AICD, APP intracellular domain; PS, presenilin; FAD, familial Alzheimer disease; NTF, N-terminal fragment; CTF, C-terminal fragment; HEK293, human embryonic kidney 293; MEFs, mouse embryonic fibroblasts; CHAPSO, 3-[(3-cholamidopropyl)dimethylammonio]-2-hydroxy-1-propanesulfonic acid; ELISA, enzyme-linked immunosorbent assay; WT, wild-type; $PS1^{LA}$, PS1 yielding longer Aβ peptides.

This paper is available on line at http://www.jbc.org

tered throughout the sequence of PSs can selectively up-regulate the enzymatic production of $A\beta_{42/43}$.

While trying to address this conundrum, we realized that the FAD-linked mutations and the few site-directed mutagenesis studies described to date (12, 16–19) did not provide an unbiased view of the effects of PS mutations on γ-secretase activity. Thus, the clinical mutations were ascertained by linkage to FAD, whereas the site-directed mutations in conserved residues were created to test specific hypotheses. We therefore undertook a screen of randomly mutagenized PS1 to identify single residue missense mutations that affect the physiological endoproteolysis of PS1 and/or selectively change Aβ isoform production. We report here the discovery and characterization of novel PS1 mutants that exclusively generate longer Aβ species, but do not support the activities for $A\beta_{40}$ generation or PS1 endoproteolysis.

EXPERIMENTAL PROCEDURES

Antibodies and Reagents—The rabbit polyclonal antibody against the N terminus of PS1 was described previously (10). Monoclonal antibodies against the PS1 CTF and APP NTF (22C11) and a polyclonal antibody against the APP CTF were purchased from Chemicon International, Inc. (Temecula, CA). Polyclonal anti-nicastrin (N1660) and monoclonal anti-FLAG tag (M2) antibodies were from Sigma. Monoclonal antibodies against p115 and the Myc tag (9E10) were obtained from BD Biosciences and Santa Cruz Biotechnology, Inc. (Santa Cruz, CA), respectively. Cycloheximide, DFK167 and sulindac sulfide were purchased from Sigma, Enzyme Systems Products (Livermore, CA), and Wako (Osaka, Japan), respectively.

Cell Culture and cDNA Transfection—Human embryonic kidney 293 (HEK293) cells and mouse embryonic fibroblasts (MEFs) derived from PS1/PS2 double knockout mice (PS-null MEFs) (20) were cultured in Dulbecco's modified Eagle's medium supplemented with 10% fetal bovine serum and 1% streptomycin/penicillin. cDNA transfection was carried out using Lipofectamine Plus reagent (Invitrogen).

Generation and Screening of a Randomly Mutagenized PS1 cDNA Library—Random mutagenesis of PS1 cDNA was performed by error-prone PCR with the forward primer 5′-TTTTGAATTCTCCTTAGACAGCTTGGCCTGGAG-3′ (corresponding to the 5′-untranslated region of human PS1 cDNA and containing an EcoRI restriction site) and the reverse primer 5′-TTTTCTCGAGACCTTTGTCCTCCCCAGATTTGG-3′ (corresponding to the 3′-untranslated region and containing an XhoI site). PCR conditions were determined for low frequency mutagenesis according to the manufacturer's instructions (Stratagene, La Jolla, CA). By sequencing 10 PCR products, we confirmed that the number of nucleotide substitutions per PS1 cDNA ranged from zero to seven. Mutagenized PS1 cDNA fragments obtained from four different PCRs were cloned into the EcoRI/XhoI sites of pCMV-script (Stratagene). Site-directed mutagenesis for subsequent confirmatory experiments was carried out using the QuikChange mutagenesis kit (Stratagene) and appropriate synthesized oligonucleotide primers. For screening for endoproteolysis-impaired mutants, PS-null MEFs were transfected with each mutagenized PS1 cDNA. At 48 h after transfection, cells were harvested and homogenized in a Teflon/glass homogenizer. Crude membrane fractions were isolated from the post-nuclear supernatants by centrifugation at 12,000 × *g* for 30 min and then subjected to Western analysis with anti-PS1 antibody.

Retrovirus-mediated Gene Expression—The retroviral infection of PS-null MEFs was carried out as described (21). Briefly, PLATE-E packaging cells were transfected with a retroviral vector (pMXs) carrying the cDNA encoding PS1 or human APP using FuGENE 6 (Roche Diagnostics). Culture media collected 2 days after transfection were used for viral stocks. For infection, MEFs were incubated with viral stock containing 10 μg/ml Polybrene (Sigma) for 6 h. One day after infection, the medium was replaced with fresh Dulbecco's modified Eagle's medium supplemented with 10% fetal bovine serum and 1% streptomycin/penicillin, and the MEFs were cultured for another 48 h for the preparation of conditioned medium to be used in Aβ measurements. The infection efficiency was >95% in this study, estimated by a control experiment using pMXs-GFP, carrying cDNA for jellyfish green fluorescent protein.

Immunoprecipitation and Western Analysis—Cells or membrane fractions were lysed in lysis buffer (25 mM HEPES (pH 7.5), 150 mM NaCl, 2 mM EDTA, and 10% glycerol) containing 1% Nonidet P-40 and protease inhibitor mixture (Roche Diagnostics). Western blotting was performed as described previously (10). For immunoprecipitation, cells were lysed in lysis buffer containing 1% CHAPSO. After preclearing with protein A-Sepharose CL-4B (Amersham Biosciences AB, Uppsala, Sweden), cell lysates were incubated with antibody for 2 h, followed by overnight incubation with protein A-Sepharose at 4 °C. The immunoprecipitates were washed three times with 1% CHAPSO buffer and analyzed by Western blotting.

Glycerol Velocity Gradient Centrifugation—Glycerol velocity gradient centrifugation was carried out as described previously (22). HEK293 cells transfected with PS1 cDNA were disrupted with a Polytron homogenizer (Kinematica AG, Littau-Lucerne, Switzerland), and nuclei and large cell debris were sedimented by centrifugation at 1500 × *g* for 10 min. The post-nuclear supernatants were centrifuged at 100,000 × *g* for 1 h in a Beckman ultracentrifuge to prepare crude membrane fractions. After solubilization in lysis buffer containing 1% CHAPSO, membrane fractions were applied to the top of 15–30% (w/v) linear glycerol gradients. The gradients were centrifuged at 36,000 × *g* for 18 h and split into 12 fractions from the bottom. The fractionated proteins were analyzed by Western blotting. Ferritin (440 kDa), β-amylase (200 kDa), lactate dehydrogenase (140 kDa), and bovine serum albumin (67 kDa) were used as molecular mass markers.

Evaluation of PS-dependent Cleavages of APP and Notch—For analysis of AICD generation, crude membrane fractions were obtained from HEK293 cells expressing various PS1 mutants and solubilized in lysis buffer containing 0.5% CHAPSO and 5 mM 1,10-phenanthroline (Sigma). The lysates were incubated for 1 h at 37 °C and analyzed by Western blotting. For assessment of Notch intracellular domain generation, HEK293 cells expressing the PS1 mutant were transiently transfected with NotchΔE tagged with Myc epitopes (23). After starvation in Met-free medium, cells were metabolically labeled for 20 min with 500 μCi/ml [^{35}S]Met (ICN Biomedicals) and then incubated for 1 h in complete Dulbecco's modified Eagle's medium supplemented with 10% fetal bovine serum. Cell lysates were immunoprecipitated with anti-Myc antibody and separated by polyacrylamide gel electrophoresis. Secreted Aβ levels were measured by enzyme-linked immunosorbent assays (ELISAs) specific for $A\beta_{40}$ or $A\beta_{42/43}$ as described (24).

Immunoprecipitation/Mass Spectrometry Analysis—Immunoprecipitation/mass spectrometry analysis of Aβ peptides was performed as described previously (4). Secreted Aβ peptides in conditioned media were immunoprecipitated with monoclonal antibody 4G8 (Senetek, Napa, CA) using protein A/G Plus-agarose beads (Santa Cruz Biotechnology, Inc.). Aβ peptides were analyzed by matrix-assisted laser desorption ionization time-of-flight mass spectrometry using a Voyager-DE STR mass spectrometer (Applied Biosystems, Foster City, CA). Each mass spectrum was averaged from 1000 measurements and calibrated with bovine insulin as an internal calibrant.

Immunocytochemistry—Cells were fixed with 4% paraformaldehyde for 15 min and then permeabilized with 0.1% Triton X-100 for 5 min. Nonspecific antibody binding was blocked by incubating cells with 5% normal goat serum for 1 h. For double staining, fixed cells were incubated overnight at 4 °C with a mixture of primary antibodies, followed by reaction for 2 h with Alexa Fluor 594-conjugated anti-rabbit and Alexa Fluor 488-conjugated anti-mouse secondary antibodies (Molecular Probes, Inc.). The slides were analyzed with an LSM510 confocal laser scanning microscope (Carl Zeiss, Oberkochen, Germany).

Subcellular Fractionation with Discontinuous Sucrose Gradients—Subcellular fractionation was performed according to a previously described method (22). HEK293 cells transfected with PS1 cDNA were homogenized with a Polytron homogenizer in 5 mM HEPES (pH 7.2), 1 mM EDTA, and protease inhibitor mixture. The post-nuclear supernatant was obtained by centrifugation at 1000 × *g* for 10 min and loaded on the top of a discontinuous sucrose gradient (1 ml/2.0 M, 3.4 ml/1.3 M, 3.4 ml/1.0 M, and 2.7 ml/0.6 M) made up in the same buffer. The gradient was centrifuged for 2 h at 280,000 × *g* in a Beckman ultracentrifuge, and 24 fractions were collected from the bottom of the tube with a peristaltic pump. Fractions were trichloroacetic acid-precipitated, and proteins were analyzed by Western blotting.

RESULTS

Identification of Novel Endoproteolysis-impaired PS1 Mutants by Random Mutagenesis Screening—We generated and screened a randomly mutagenized PS1 cDNA library to identify mutants that were defective in PS1 endoproteolysis. We isolated 370 clones that were then transiently transfected into PS-null MEFs. Upon Western analysis, 33 of the PS1 mutants displayed impaired PS1 endoproteolysis. DNA sequencing re-

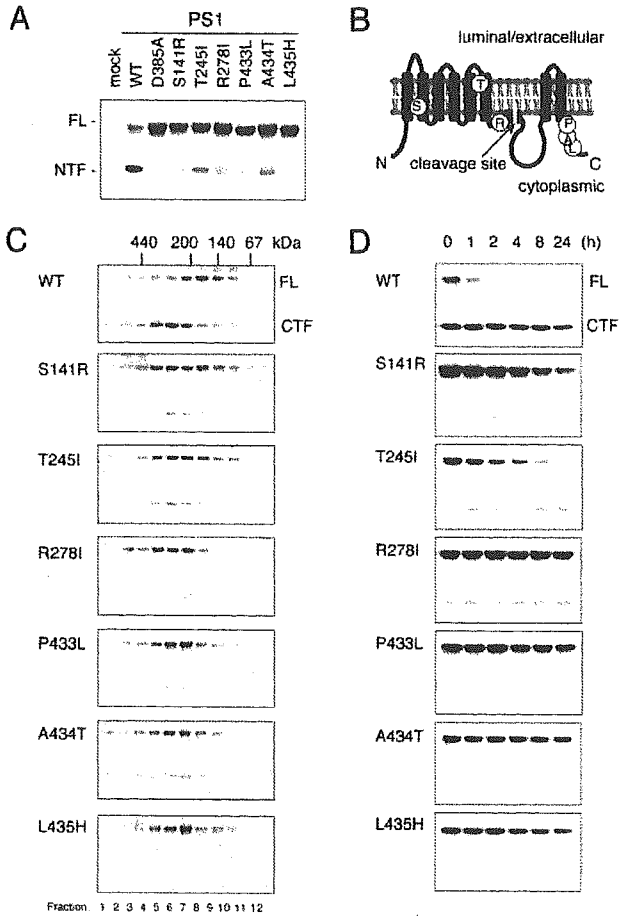

FIG. 1. **Endoproteolysis-impaired missense mutant PS1 proteins form stable high molecular mass complexes.** *A*, the impaired endoproteolysis of mutant PS1 proteins is shown. The membrane fraction from PS-null MEFs transiently transfected with each PS1 mutant was immunoblotted with anti-PS1 antibody. WT-PS1 and the loss-of-function mutant D385A-PS1 served as controls. *FL*, full-length. *B*, the scheme shows the locations of mutated residues in PS1 mutants in the eight-TM model. *C*, glycerol velocity gradient fractions of CHAPSO lysates from PS1-transfected HEK293 cells were analyzed for PS1. The positions of molecular mass markers are indicated at the top. Results are representative of three independent experiments. *D*, after treatment with 25 μg/ml cycloheximide for the indicated times, the lysate from HEK293 cells stably expressing each PS1 mutant was detected using anti-PS1 antibody.

vealed that seven of these mutants had nonsense mutations. The remaining 26 mutants harbored missense mutations that were located throughout the molecule (data not shown). Six of these 26 mutants contained single amino acid substitutions: S141R, T245I, R278I, P433L, A434T, and L435H (Fig. 1, *A* and *B*). Ser^{141} and Thr^{245} are located within the second and sixth TM domains, respectively, and are not conserved in homologs of *Caenorhabditis elegans*. Arp^{278} is a conserved residue at the N terminus of the cytoplasmic loop between the sixth and seventh TM domains, and Pro^{433}, Ala^{434}, and Leu^{435} are located in the highly conserved PAL motif in the cytoplasmic C-terminal tail (17).

Mutant PS1 Proteins Form Stable High Molecular Mass Complexes—To assess the functional properties of these PS1 mutants, each was stably transfected into HEK293 cells that also expressed a construct equivalent to the C-terminal β-secretase-processed APP fragment C99, which is the immediate substrate for γ-secretase and yields Aβ. Because functional endoproteolytic derivatives of wild-type (WT) PS1 assemble into a stable high molecular mass complex (22), we initially investigated 1) the incorporation of each mutant into macromolecular complexes, 2) the ability of each mutant to replace endogenous PS1, and 3) the metabolic half-life of each mutant protein. Glycerol velocity gradient analyses revealed that the uncleaved mutant holoproteins were assembled into high molecular mass complexes that were of similar size as the endogenous complexes (~200–400 kDa), although the complexes containing the S141R and T245I mutants were also distributed broadly in the lower molecular mass ranges (Fig. 1*C*). The mutant holoproteins also displaced the proteolytic fragments of endogenous presenilins (Fig. 1*C*). Reciprocal co-immunoprecipitation assays confirmed that, similar to WT-PS1, all six PS1 mutants bound to the other γ-secretase components (nicastrin, APH-1, and PEN-2) (data not shown). As shown in Fig. 1*D*, the half-lives of the mutant holoproteins in the presence of cycloheximide were comparable with those of WT proteolytic fragments ($t_{1/2}$ > 24 h) and were much longer than the half-life of the WT holoprotein ($t_{1/2}$ < 1 h). The S141R-PS1 and T245I-PS1 holoproteins were less well stabilized ($t_{1/2}$ = ~8 and ~4 h, respectively). Taken together, all six mutations specifically prevented PS1 endoproteolysis, but did not significantly impede the assembly and stabilization of mutant PS1 complexes.

Proteolytic Activities of PS1 Mutants—To investigate the ability of these mutants to support γ- and ε-cleavage of APP, we measured the production of AICD and Aβ from HEK293 cell lines expressing mutant PS1 and APP fragment C99. In comparison with cells expressing WT-PS1, the generation of AICD was clearly suppressed in all six mutant cell lines (Fig. 2*A*). Similarly, S3 cleavage of Notch, which corresponds to ε-cleavage of APP, was clearly attenuated (Fig. 2*B*). An ELISA specific for $Aβ_{40}$ or $Aβ_{42/43}$ revealed that the level of $Aβ_{40}$ secreted from mutant PS1-expressing cells was either comparable with or lower than the level of $Aβ_{40}$ secreted from WT-PS1 cells (Fig. 2*C*). In contrast, the level of secreted $Aβ_{42/43}$ was significantly elevated in five of the six mutant cell lines. Finally, P433L-PS1 cells secreted less $Aβ_{40}$ and $Aβ_{42/43}$ than WT-PS1 cells. These mutants exhibited dominant phenotypes for the secretion of $Aβ_{40}$ and $Aβ_{42/43}$ presumably through the replacement of endogenous PSs.

To assess the γ-secretase activity of these mutants in the absence of endogenous PSs, we transfected each of these PS1 mutants together with human APP into PS-null MEFs using retroviral vectors and then measured Aβ levels in the conditioned media from these cells (Fig. 3*A*). Transfection of WT-PS1 successfully restored Aβ secretion, whereas compared with transfection with WT-PS1, transfection of FAD-causing mutants (I143F-PS1 and L392V-PS1) led to Aβ secretion with an increased ratio of $Aβ_{42/43}$ to total Aβ. The P433L mutant did not restore Aβ secretion, supporting the idea that P433L is a loss-of-function mutation (17, 25). In contrast, the five other mutants secreted significant amounts of $Aβ_{42/43}$ while secreting only minimum or background levels of $Aβ_{40}$. Because the R278I and L435H mutants generated particularly high levels of $Aβ_{42/43}$, we focused on these mutants in the following experiments.

To reveal the profile of Aβ species secreted by MEFs expressing R278I-PS1 or L435H-PS1, we performed immunoprecipitation/mass spectrometry as described previously (4). The spectrum of matrix-assisted laser desorption ionization time-of-flight mass spectrometry indicated that the Aβ species secreted by these MEFs always ended at Thr^{43} (*i.e.* Aβ-(11–43) and Aβ-(1–43)) (Fig. 3*B*). These mutants are quite unique in exclusively generating $Aβ_{43}$ and are therefore designated $PS1^{LA}$ for PS1 yielding longer Aβ peptides.

The R278I and L435H mutations are located in the NTF and

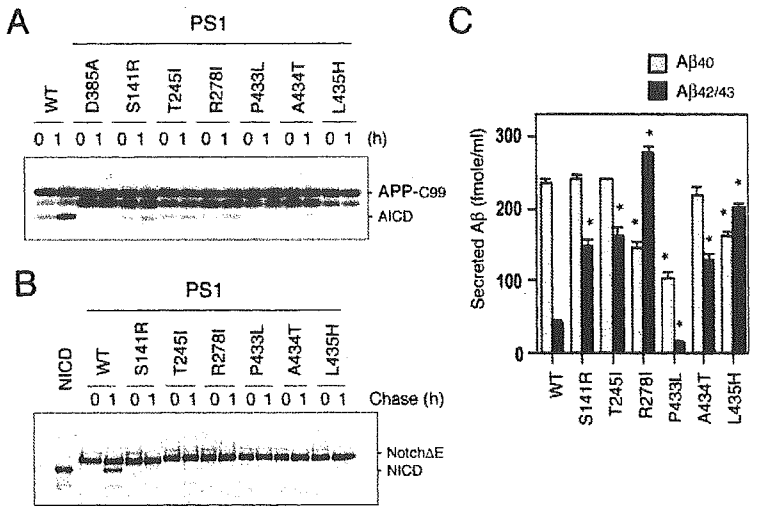

FIG. 2. **PS-dependent protease activities in mutant PS1-expressing HEK293 cells.** *A*, ε-cleavage in cells stably expressing mutant PS1 and APP fragment C99. AICD fragments generated from 0.5% CHAPSO-extracted membrane fractions were evaluated by immunoblotting with anti-APP antibody. WT-PS1 and the loss-of-function mutant D385A-PS1 served as controls. Results are representative of at least three independent experiments. *B*, S3 cleavage of Notch in mutant PS1-expressing cells. After transient transfection with NotchΔE-Myc, mutant PS1-expressing cells were metabolically pulse-labeled and chased for 1 h. Immunoprecipitates with anti-Myc antibody were analyzed by polyacrylamide gel electrophoresis. An autoradiograph of the dried gel is shown. *NICD*, Notch intracellular domain. *C*, Aβ secretion from cells expressing WT-PS1 or mutant PS1. $Aβ_{40}$ and $Aβ_{42/43}$ levels in conditioned media were quantified by ELISA. Data represent the means ± S.D. (n = 3). *, $p < 0.001$ by one-way analysis of variance with Dunnett's post-hoc test compared with the values in WT-PS1 cells.

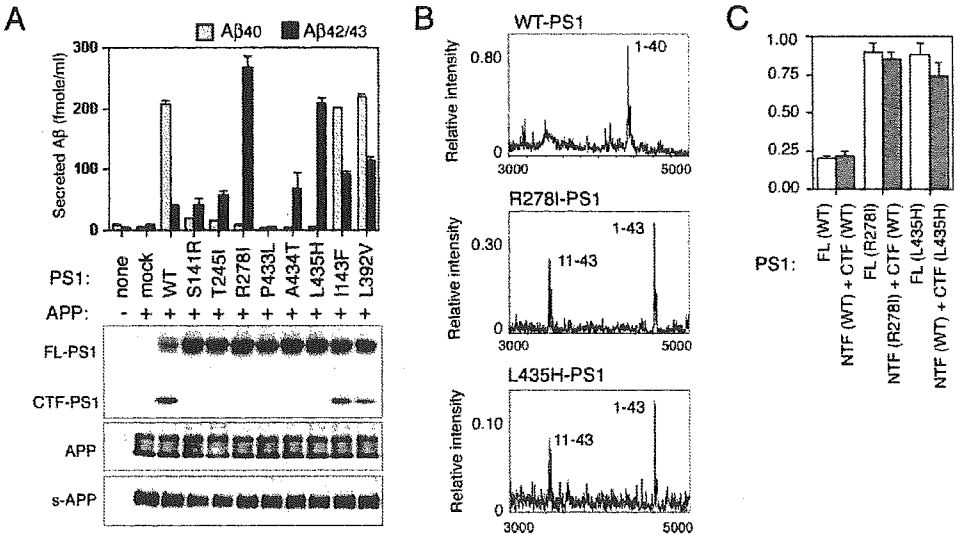

FIG. 3. **γ-Secretase activities of PS1 mutants on a PS-null background.** *A*, secreted Aβ levels from PS-null MEFs transfected with PS1 mutants were measured. PS-null MEFs were retrovirally cotransfected with PS1 and APP, and secreted Aβ levels were measured by ELISA. Data represent the means ± S.D. (n = 3). The immunoblots for transfected PS1, APP, and the secreted APP ectodomain (*s-APP*) are shown. *FL*, full-length. *B*, the profile of Aβ species secreted from PS-null MEFs transfected with WT-PS1, R278I-PS1, or L435H-PS1 was analyzed by immunoprecipitation/mass spectrometry. *C*, secreted Aβ levels from PS-null MEFs cotransfected with human APP and the indicated PS1 constructs were measured by ELISA. The ratios of $Aβ_{42/43}$ to total Aβ are shown. Data represent the means ± S.D. (n = 3).

CTF of PS1, respectively (Fig. 1*B*). To determine whether these mutations might have cooperative or additive effects, we generated a PS1 cDNA harboring both mutations in *cis*. When expressed in PS-null MEFs, this double mutant formed a holoprotein that was incorporated into stable high molecular mass complexes, but rescued neither $Aβ_{40}$ nor $Aβ_{42/43}$ secretion (data not shown). This suggests that the double $PS1^{LA}$ mutation causes a loss of γ-secretase activity and that $PS1^{LA}$ is an incomplete loss-of-function mutation.

PS1 endoproteolysis is thought to occur during PS1 complex maturation and prior to the activation of γ-secretase (13). To exclude the possibility that the inefficient endoproteolysis of the mutant holoproteins had affected the cleavage specificity of γ-secretase, we simulated endoproteolysis of the mutant proteins by co-infecting PS-null MEFs with two cDNAs: one encoding the PS1 NTF (residues 1–291) and the other encoding the PS1 CTF (residues 292–467). In both cases, the R278I and L435H mutations were contained in the appropriate hemiconstructs. The amounts of total Aβ (data not shown) and the ratios of $Aβ_{42/43}$ to total Aβ produced in these experiments were comparable with those produced in PS-null MEFs infected with the corresponding full-length cDNA (Fig. 3*C*). In addition, coexpression of the PS1 NTF and CTF harboring R278I and L435H mutations, respectively, did not restore Aβ secretion (data not shown). These results confirm that γ-secretase activity was modified by the specific

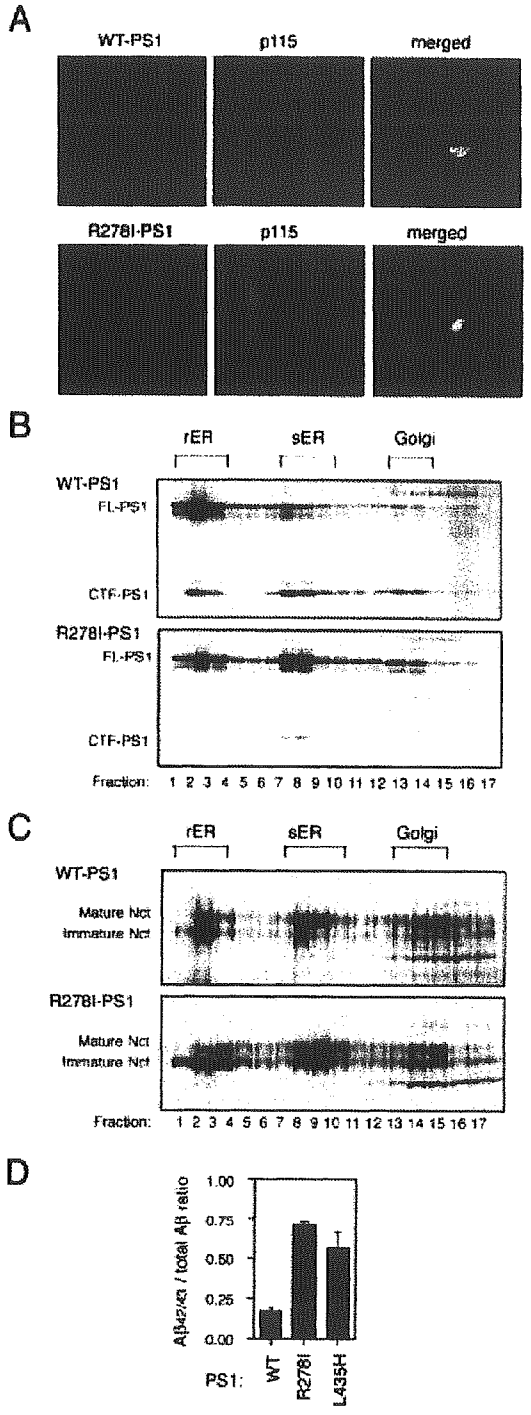

FIG. 4. **Subcellular localization of PS1 and cleavage specificity of γ-secretase.** *A*, PS-null MEFs retrovirally transfected with WT-PS1 or R278I-PS1 were investigated by immunocytochemistry. Immunoreactivities for the PS1 CTF and the Golgi marker protein p115 are shown in *red* and *green*, respectively. The merged images show the localization of PS1 in the Golgi apparatus as *yellow* fluorescence. *B* and *C*, HEK293 cells stably transfected with WT-PS1 or R278I-PS1 were fractionated by sucrose density centrifugation. The fractionated proteins were analyzed by immunoblotting with anti-PS1 (*B*) or anti-nicastrin (*Nct*) (*C*) antibody. *FL*, full-length; *rER*, rough endoplasmic reticulum; *sER*, smooth endoplasmic reticulum. *D*, Aβ generated in cell-free systems in CHAPSO lysates of membrane fractions from HEK293 cells overexpressing WT-PS1 and mutant PS1 was assessed by ELISA. The ratios of $Aβ_{42/43}$ to total Aβ are shown. Data represent the means ± S.D. (n = 3).

amino acid substitution rather than due to the lack of endoproteolysis of the mutant holoprotein.

The R278I Mutation Does Not Alter the Subcellular Localization of the PS1 Protein—Previous studies have suggested that $Aβ_{40}$ and $Aβ_{42/43}$ arise from γ-secretase cleavage at distinct subcellular locations (26–28). However, three observations argue that simple mistrafficking of the $PS1^{LA}$ mutants is not the reason for $Aβ_{42/43}$ production. First, there were no significant differences in the subcellular distribution of the WT-PS1 CTF and the R278I-PS1 holoprotein in immunocytochemical experiments or upon subcellular fractionation with sucrose gradients (Fig. 4, *A* and *B*). Both PS1 species appeared to be similarly transported from the endoplasmic reticulum to the Golgi apparatus. Second, the pattern of nicastrin glycosylation in R278I-PS1-expressing cells was indistinguishable from that in WT-PS1-expressing cells (Fig. 4*C*). Finally, the selective overproduction of $Aβ_{42/43}$ by R278I-PS1 or L435H-PS1 cells was still evident even when Aβ peptides were generated in a solubilized membrane fraction prepared from these cells (Fig. 4*D*).

Different Amino Acid Substitutions at the Same Residue Can Result in Distinct Modifications of γ-Secretase Activity—The R278I mutation conferred exclusive generation of $Aβ_{43}$, whereas the P433L mutation resulted in loss of function. To address whether these substitutions have a specific role in PS1 endoproteolysis and γ-secretase activities, we generated and tested additional mutations at these residues. We introduced five other mutations into the R278 codon, including the FAD-linked R278K and R278T mutations as well as substitutions of Ser, Glu, and Pro, which have polar, negatively charged, and imino group side chains, respectively. Unlike the R278I mutation, all of these substitutions increased the level of secreted $Aβ_{42/43}$, but did not affect either PS1 endoproteolysis or $Aβ_{40}$ secretion (Fig. 5*A*).

Next, we generated seven mutations at Pro^{433} and tested γ-secretase activity (Fig. 5*B*). Similar to P433L-PS1, mutant PS1 bearing a substitution of Pro^{433} with Ile, Glu, Lys, or Gln was not cleaved and could not restore Aβ secretion when expressed in PS-null MEFs. In contrast, but similar to $PS1^{LA}$ mutations, the P433S and P433G mutations caused impaired self-endoproteolysis, reduced $Aβ_{40}$ secretion, and enhanced $Aβ_{42/43}$ generation. Finally, like the FAD-linked mutants, P433A-PS1 was cleaved normally and exhibited a high ratio of $Aβ_{42/43}$ to total Aβ. A434C and L435F (FAD-linked mutations at the neighboring residues of Pro^{433}) caused enhanced secretion of $Aβ_{42/43}$ (data not shown); and, very recently, A434D and L435R were reported to be loss-of-function mutations (25). Altogether, these results indicate that different amino acid substitutions at the same residue can result in distinct modifications of γ-secretase activity.

Pharmacological Assessment of $PS1^{LA}$ Mutant-associated Protease Activities—In addition to mutations of PSs and APP, γ-secretase inhibitors are also known to modulate the ratio of $Aβ_{42/43}$ to total Aβ (29–31). Previous reports have shown that FAD-linked mutations attenuate the effect of γ-secretase inhibitors (32–34); however, these data were obtained with cells expressing both WT-PS1 and mutant PS1. We therefore re-evaluated the effects of γ-secretase inhibitors using MEFs expressing a single genotype of PS1. The results in Fig. 6*A* confirm previous reports (30, 35, 36) and show that, in MEFs expressing WT-PS1, the peptidomimetic difluoroketone inhibitor DFK167 selectively enhanced the γ-secretase activity of $Aβ_{42/43}$ generation (referred to as γ-42/43 activity) at subinhibitory doses, but inhibited the γ-secretase activity of $Aβ_{40}$ generation (referred to as γ-40 activity) in a dose-dependent manner. However, this enhancement of $Aβ_{42/43}$ secretion was